EurJIC European Journal of Inorganic Chemistry

ChemPubSoc Europe

FULL PAPER

DOI:10.1002/ejic.201301216

Yellow-Emitting $Sr_9Sc(PO_4)_7$:Eu^{2+}, Mn^{2+} Phosphor with Energy Transfer for Potential Application in White Light-Emitting Diodes

Xiaoling Dong,[a,b] Jiahua Zhang,*[a] Liangliang Zhang,[a,b] Xia Zhang,[a] Zhendong Hao,[a] and Yongshi Luo[a]

Keywords: Luminescence / Light-emitting diodes / Energy transfer / Manganese / Europium

Eu^{2+}–Mn^{2+} codoped yellow-emitting $Sr_9Sc(PO_4)_7$ (SSP) phosphors have been synthesized by solid-state reactions. The synthesis, structure refinement, and luminescence properties of the obtained phosphor were investigated in detail. The obtained phosphor exhibits a strong excitation band between 250 and 450 nm, matching well with the dominant emission band of a near-UV light-emitting-diode (LED) chip. Upon excitation at 365 nm, the $Sr_9Sc(PO_4)_7$:Eu^{2+}, Mn^{2+} phosphor shows strong yellow emissions centered at 510 and 610 nm. The energy transfer mechanism from Eu^{2+} to Mn^{2+} in $Sr_9Sc(PO_4)_7$:Eu^{2+}, Mn^{2+} has been studied and demonstrated to be a resonant type through a dipole-quadrupole mechanism based on the decay lifetime data. These results indicate that yellow-emitting $Sr_9Sc(PO_4)_7$:Eu^{2+}, Mn^{2+} can serve as a promising candidate for application in white-light LEDs.

Introduction

White light-emitting diodes (LEDs) have attracted much attention due to their high luminous efficiency, good material stability, long lifetime, and energy savings.[1–4] The applications of these LEDs include lighting sources and backlit automobile lamps.[5–7] Nowadays, the most dominant way to create a white LED is by combining a blue InGaN chip with $Y_3Al_5O_{12}$:Ce^{3+}(YAG:Ce)-based yellow phosphors.[8–10] However, because of the deficient emission in the red spectral region, this approach generates a cool white light that is unsuitable for room lighting. Therefore, the lack of a red-light component restricts their use in more vivid applications.[11,12] Recently, white LEDs fabricated using near-UV chips (380–420 nm) coupled with a blend of yellow- and blue-emitting phosphors have exhibited favorable properties, including tunable correlated color temperature (CCT), tunable Commission International de l'Eclairage (CIE) chromaticity coordinates, and an excellent color rendering index (CRI). Therefore, the development of new yellow-emitting phosphors that can be effectively excited in the NUV range is a very important prospect that requires prompt attention. Many yellow-emitting phosphors for NUV LEDs have been identified and investigated, for example, $Ba_2Gd(BO_3)_2Cl$:Eu^{2+},[13] $Ba_2Mg(BO_3)_2$:Eu^{2+},[14] $Ba_3Gd(PO_4)_3$:Eu^{2+}, Mn^{2+}.[15]

At present, increasing attention has been focused on the development of luminescent materials based on phosphate hosts because of their easy-synthesis, high luminous efficiency, and excellent thermal stability.[16–18] Recently, a variety of compounds that are structurally similar to $Sr_9A(PO_4)_7$ have been reported in the literature, such as $Sr_8MgSc(PO_4)_7$,[19] $Sr_8MgGd(PO_4)_7$,[20] and $Sr_8ZnSc(PO_4)_7$.[21] These materials exhibit excellent photoluminescence properties for application in white LEDs. To the best of our knowledge, the crystal structures and luminescence properties of $Sr_9Sc(PO_4)_7$:Eu^{2+}, Mn^{2+} have not yet been reported in the literature. In this study, we have demonstrated the crystal structure of the $Sr_9Sc(PO_4)_7$ phosphor and investigated the luminescence properties of yellow-emitting $Sr_9Sc(PO_4)_7$:Eu^{2+}, Mn^{2+} phosphors. Moreover, the energy-transfer mechanism between the Eu^{2+} and Mn^{2+} ions in the host has been analyzed through the fluorescence decay curves.

Results and Discussion

Phase Identification and Crystal Structure

The experimental (crosses), calculated (solid line), and difference (bottom) XRD profiles for the Rietveld refinement of SSP:0.03Eu^{2+} are shown in Figure 1. The initial structure model that approximates the actual structure of SSP:0.03Eu^{2+} was constructed with crystallographic data previously reported for $Sr_9In(PO_4)_7$.[22] SSP:0.03Eu^{2+} crys-

[a] Key Laboratory of Luminescence and Application, Changchun Institute of Optics, Fine Mechanics and Physics, Chinese Academy of Sciences,
Changchun 130033, P. R. China
E-mail: zhangjh@ciomp.ac.cn
http://yjs.ciomp.ac.cn:8004/sys02/
[b] Graduate School of Chinese Academy of Sciences,
Beijing 100049, China

tallizes in a monoclinic unit cell with space group *I*2/*a* and lattice constants a = 18.02194(15) Å, b = 10.65529(8) Å, c = 18.35774(14) Å, β = 132.93622(32)°, and V = 2580.855(36) Å^3. The refinement finally converged to R_p = 2.69%, R_{wp} = 3.51%, R_{exp} = 2.45%, and χ^2 = 2.05 shown in Table 1. The Sr^{2+} ions have five different sites in SSP compounds, which are coordinated to either eight or nine oxide ions. Sr^{2+} ions at the Sr4 site are disordered over two positions near a center of symmetry. The ionic radii for eight- and nine-coordinate Sr^{2+} are 1.26 and 1.31 Å, respectively. However, the ionic radii for eight- and nine-coordinated Eu^{2+} are 1.25 and 1.3 Å, respectively, and that for eight-coordinate Mn^{2+} is 0.96 Å. On account of the matching of ionic radii and ionic valence, we have proposed that Eu^{2+} and Mn^{2+} are expected to randomly occupy the Sr^{2+} ion sites in the host structure.

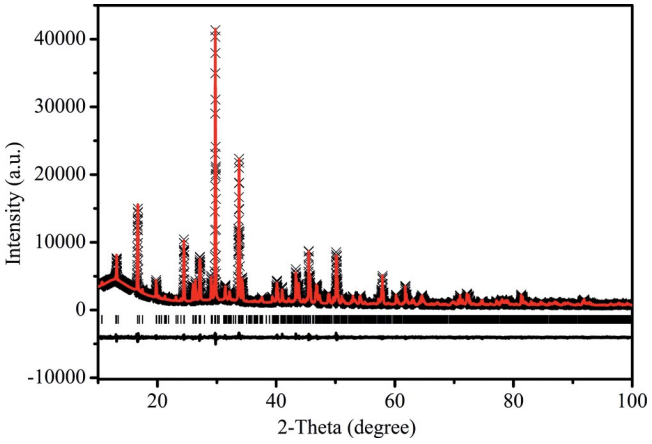

Figure 1. The experimental (crosses), calculated (solid line), and difference results (bottom) of the XRD refinement of SSP:0.03Eu^{2+}.

Table 1. Rietveld refinement and crystal data of $Sr_9Sc(PO_4)_7$ phosphor.

Empirical formula	$Sr_9Sc(PO_4)_7$
Radiation type [Å]	1.54056
2θ range [°]	10–100
Symmetry	monoclinic
Space group	*I*2/*a*
a [Å]	18.02194(15)
b [Å]	10.65529(8)
c [Å]	18.35774(14)
β [°]	132.93622(32)
V [Å^3]	2580.855(36)
Z	4
R_p [%]	2.69
R_{wp} [%]	3.51
R_{exp} [%]	2.45
χ^2	2.05

Photoluminescence Properties

Figure 2 (a) illustrates the PLE and PL spectra of the SSP:0.03Eu^{2+} sample. Upon 365 nm excitation the PL spectrum exhibits a broad emission band peak at 510 nm, which is attributed to the $4f^65d^1$–$4f^7$ transition of the Eu^{2+} ions. The broad asymmetric PL spectrum implies that the emission spectrum consists of several broad bands, which are ascribed to Eu^{2+} occupying different cation sites in the SSP lattice. The luminescence of Eu^{3+} in the PL spectrum also exists. The reason may be that Eu^{3+} ions occupy some sites that make Eu^{3+} ions difficult to reduce to Eu^{2+} ions. Figure 2 (b) shows the PLE and PL spectra of the SSP:0.10Mn^{2+} sample. The PLE spectrum (330–500 nm) shows several bands centered at 344, 355, and 404 nm, which are assigned to the transitions from $^6A_1(^6S)$ to $^4E(^4D)$, $^4T_2(^4D)$, and [$^4A_1(^4G)$, $^4E(^4G)$] levels of Mn^{2+}, respectively.[23] The PL spectrum shows a broad emission band centered at 610 nm ascribed to the spin-forbidden $^4T_1(^4G)$–$^6A_1(^6S)$ transition of the Mn^{2+} ions.

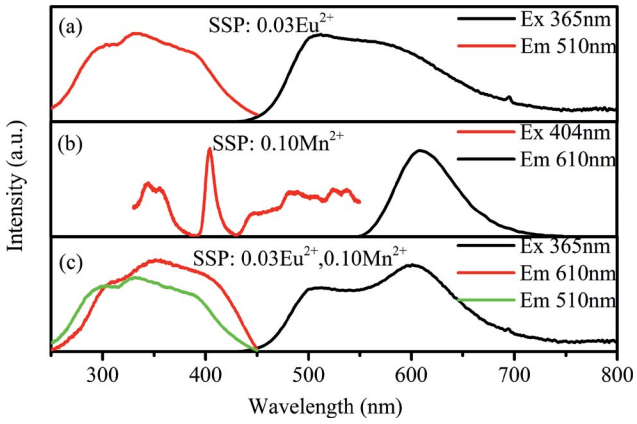

Figure 2. PL and PLE spectra for SSP:0.03Eu^{2+} (a), SSP:0.10Mn^{2+} (b), and SSP:0.03Eu^{2+}, 0.10Mn^{2+} (c).

As shown in Figure 2 (a) and Figure 2 (b), there is a substantial spectral overlap between the emission band of the Eu^{2+} ions and the excitation band of the Mn^{2+}, indicating a favorable condition for possible energy transfer between the sensitizer Eu^{2+} and the activator Mn^{2+} in the SSP host. Moreover, Figure 2 (c) shows further evidence for the energy transfer in that the PLE spectrum monitored for the emission of Mn^{2+} is consistent with that monitored for the emission of Eu^{2+}.[24] Upon excitation at 365 nm, the PL spectrum of the SSP:0.03Eu^{2+}, 0.10Mn^{2+} phosphor appears not only as a yellowish-green band from the Eu^{2+} ions but also as a red band from the Mn^{2+} ions. Therefore, we can adjust the relative intensity of the emission bands by tuning the amount of Mn^{2+} ions, and multicolor emission can be obtained in a single host through the principle of energy transfer. Accordingly, a series of samples have been prepared. The Eu^{2+} content is fixed at 0.03, whereas the Mn^{2+} content is varied from 0 to 0.30. Figure 3 shows the emission spectra of the SSP:0.03Eu^{2+}, $x$$Mn^{2+}$ phosphors (x = 0, 0.05, 0.10, 0.20, 0.30) under 365 nm excitation. The intensity of Eu^{2+} yellowish-green emission decreases monotonically with increasing Mn^{2+} content. In contrast, the intensity of Mn^{2+} red emission increases gradually until the Mn^{2+} concentration is above 0.10. The apparent decrease in the PL intensity for Mn^{2+} with $x > 0.10$ is primarily due to the concentration quenching effect.

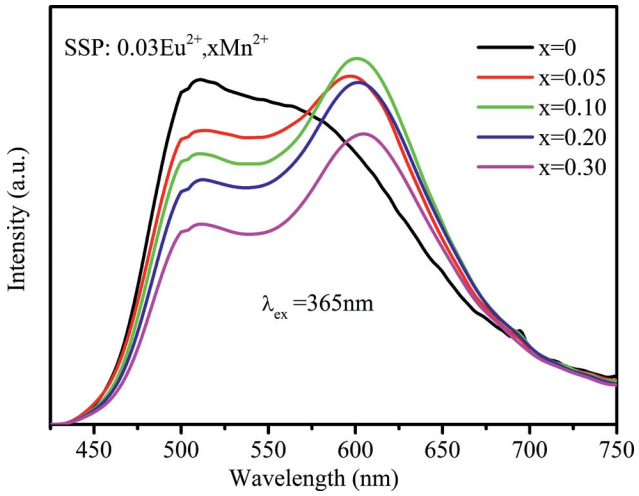

Figure 3. PL spectra of SSP:0.03Eu^{2+}, $x$$Mn^{2+}$ phosphors with different doping contents x at the excitation wavelength of 365 nm.

The fluorescent decay curves of the Eu^{2+} ions in the SSP:0.03Eu^{2+}, $x$$Mn^{2+}$ samples were measured by monitoring the emission of the Eu^{2+} ions at 510 nm as presented in Figure 4. One can see that the decay curves of the Eu^{2+} ions deviate slightly from a single exponential rule at lower Mn^{2+} doping content and the deviations become more obvious with an increase in the Mn^{2+} concentration. Because all the decay curves deviate from single exponential decay, the average fluorescence lifetime was defined as the following formula [Equation (1)][25,26]

$$\tau_{avg} = \int_0^\infty I_D(t)dt \quad (1)$$

where $I_D(t)$ is the fluorescence intensity at time t with normalized initial intensity. The fluorescence lifetimes of Eu^{2+} were calculated according to Equation (1). In the SSP:0.03Eu^{2+}, $x$$Mn^{2+}$ samples, as the value of x increases

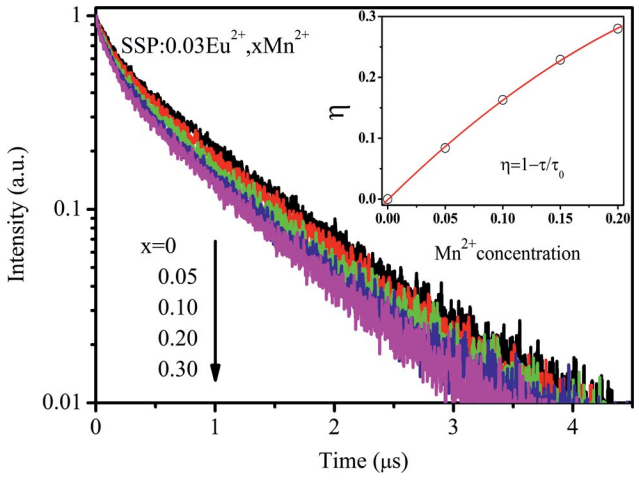

Figure 4. Decay curves of Eu^{2+} fluorescence in SSP:0.03Eu^{2+}, $x$$Mn^{2+}$ (excited at 355 nm, monitored at 510 nm). Inset: energy-transfer efficiency with different doping Mn^{2+} contents.

from 0 to 0.30, the lifetime for Eu^{2+} is found to decrease monotonically from 633, 580, 530, 488, to 456 ns, which is strong evidence for the energy transfer between Eu^{2+} and Mn^{2+}.

The energy transfer efficiency was defined as the ratio of donors that are depopulated by acceptors through energy transfer over the total number of donors that are excited in the presence of the acceptor. Assuming that all excited Mn^{2+} ions decay radiatively, the energy transfer efficiency (η_T) from Eu^{2+} to Mn^{2+} can be calculated according to the data of average lifetime by Equation (2).[27]

$$\eta_T = 1 - \tau / \tau_0 \quad (2)$$

τ and τ_0 are the decay time of the sensitizer Eu^{2+} in the presence and absence of the activator Mn^{2+}, respectively. On the basis of Equation (2), the energy transfer efficiency (η_T) was calculated and is displayed in the inset of Figure 4. The results indicate that the energy transfer efficiency from Eu^{2+} to Mn^{2+} is effective and depends strongly on the doping content of the Mn^{2+} ions in the SSP host. Obviously, it is known from the inset of Figure 4 that the energy-transfer efficiency from the Eu^{2+} to Mn^{2+} ions increases gradually with an increase in Mn^{2+} concentration.

The decay curves that deviate from single exponential decay become more obvious with an increase in the Mn^{2+} concentration x, reflecting the effect of energy transfer. Generally speaking, the energy transfer from Eu^{2+} to Mn^{2+} ions occurs through multipolar interactions. When the donor and acceptor ions are uniformly distributed in the host and the migration processes are negligible compared with the energy transfer between donors and acceptors, then the normalized intensity of the donor fluorescence decay curves follow the Inokuti–Hirayama (I–H) model equation for multipolar interactions [Equation (3)][28]

$$I_D(t) = I_{D0}(t)\exp(-Qt^{3/S}) \quad (3)$$

where $I_D(t)$ and $I_{D0}(t)$ is the decay function of donors in the presence and absence of the activator Mn^{2+}, respectively. Q is the energy-transfer parameter, τ_0 is the intrinsic decay time of the donors in the absence of acceptors. The value S = 6, 8, and 10, corresponding to dipole–dipole, dipole–quadrupole, and quadrupole–quadrupole interactions, respectively. By modifying Equation (3), the value of S can be determined from the relationship shown in Equation (4).

$$\log\left[\ln\left(\frac{I_{D0}(t)}{I_D(t)}\right)\right] \propto \log(t) \quad (4)$$

In order to get a correct S value, we plotted the decay curves using Equation (4). This plot should yield a straight line with a slope equal to 3/S. Figure 5 displays the fitting results of the SSP:0.03Eu^{2+}, $x$$Mn^{2+}$ samples. The value of S estimated from the slope was found to be 7.5, 7.69, and 8.57 for SSP:0.03Eu^{2+}, $x$$Mn^{2+}$ samples with x = 0.05, 0.20,

and 0.30, respectively. These values are nearly coincident with the conventional value of $S = 8$. This result indicates that the dominant interaction mechanism for energy transfer from Eu^{2+} to Mn^{2+} in the SSP host is based on the dipole–quadrupole interaction.

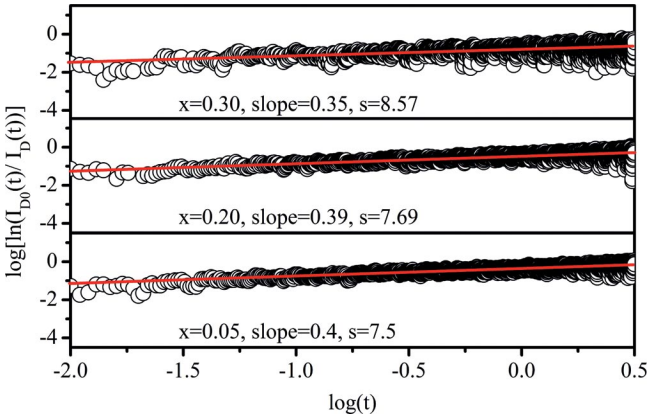

Figure 5. Plotted $\log\{\ln[I_{D_0}(t)/I_D(t)]\}$ vs. $\log(t)$ for SSP:0.03Eu^{2+}, $x$$Mn^{2+}$ phosphors.

According to the dipole–quadrupole interaction mechanism, the critical distance between Eu^{2+} and Mn^{2+} is given by spectral overlap methods [Equation (5)][29]

$$R_C^8 = 3.024 \times 10^{12} \lambda_S^2 f_q \int \frac{F_S(E)F_A(E)dE}{E^4} \quad (5)$$

where f_q is the oscillator strength of the involved absorption transition of the acceptor (Mn^{2+}), λ_S (in angstroms) is the wavelength position of the sensitizer's emission, E is the energy involved in the transfer (in eV), and $\int F_S(E)F_A(E)dE/E^4$ represents the spectral overlap between the normalized shapes of the Eu^{2+} emission $F_S(E)$ and the Mn^{2+} excitation $F_A(E)$, and in our case it is calculated to be about 0.0174 eV^{-5}. Using the above equation with $f_q = 10^{-10}$, the critical distance of energy transfer was calculated to be 10.4 Å.

Figure 6 shows the Commission Internationale de l'Eclairage (CIE) chromaticity coordinates of SSP:0.03Eu^{2+}, $x$$Mn^{2+}$ phosphors with different Mn^{2+} contents excited at 365 nm, which were calculated from the corresponding PL spectra. As the content of Mn^{2+} increased from 0 to 0.30, the corresponding color tone of the phosphor shifted from yellowish-green (A) to yellow (E). The corresponding chromaticity coordinates are listed in Table 2. Accordingly, near-UV excited white LED systems with improved chromaticity quality can be fabricated by combining near-UV LED chips with blue-emitting BAM:Eu^{2+} ($BaMgAl_{10}O_{17}$: Eu^{2+}) and our developed SSP:Eu^{2+}, $x$$Mn^{2+}$ phosphors. White light with a tunable correlated color temperature (CCT) in the region of the triangle AEK (Figure 6) can be achieved by simply adjusting the Mn^{2+} content (x) in the SSP:0.03 Eu^{2+}, $x$$Mn^{2+}$ host.

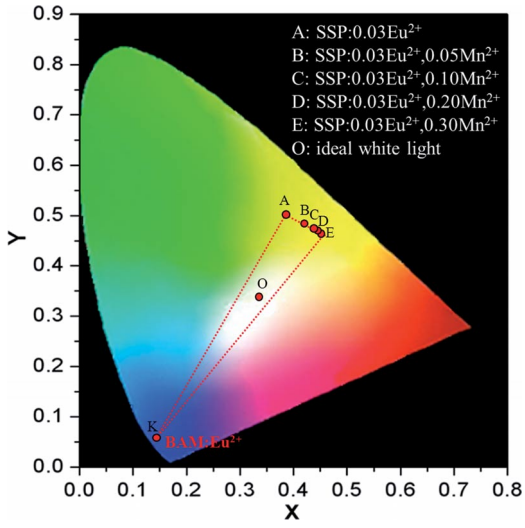

Figure 6. CIE chromaticity diagram for the SSP:0.03Eu^{2+}, $x$$Mn^{2+}$ phosphors excited at 365 nm.

Table 2. CIE chromaticity coordinates of the $Sr_9Sc(PO_4)_7$:0.03Eu^{2+}, $x$$Mn^{2+}$ samples excited at 365 nm.

Sample (x)	(x,y)
0	(0.385, 0.500)
0.05	(0.421, 0.480)
0.10	(0.437, 0.475)
0.20	(0.442, 0.473)
0.30	(0.447, 0.470)

Conclusions

In summary, we have synthesized a series of novel emission tunable SSP:Eu^{2+}, $x$$Mn^{2+}$ phosphors by a solid-state reaction. The obtained phosphor exhibits a broad excitation band in the 250–450 nm near-ultraviolet region, which matches well with near-UV chips. By adjusting the doping content ratio between Eu^{2+} and Mn^{2+}, the emission could be tuned from yellowish-green to yellow. The energy transfer from the Eu^{2+} to Mn^{2+} ions has been demonstrated to be a resonant type from a dipole–quadrupole mechanism based on the Inokuti–Hirayama model, and the energy transfer efficiency increases with an increase in Mn^{2+} concentration The critical distance was calculated as 10.4 Å. These results indicate that SSP:Eu^{2+}, $x$$Mn^{2+}$ phosphors may be used as yellow components in the fabrication of white LEDs excited by near-UV LED chips.

Experimental Section

Materials and Synthesis: The $Sr_{8.97-x}Sc(PO_4)_7$ (SSP):0.03Eu^{2+}, $x$$Mn^{2+}$ phosphors were synthesized by a high-temperature solid-state reaction. The constituent oxides or carbonates $SrCO_3$ (99.9%), Sc_2O_3 (99.9%), $(NH_4)_2HPO_4$ (99.9%), Eu_2O_3 (99.99%), and $MnCO_3$ (99.99%) were employed as the raw materials. The starting materials were thoroughly ground in an agate mortar, and the homogeneous mixture was transferred to an alumina crucible and calcined in a furnace at 1400 °C for 4 h under a reducing atmosphere of 5% H_2/95% N_2.

Measurements and Characterization: Powder X-ray diffraction (XRD) data were collected using Cu-K_a radiation (λ = 1.54056 Å) with a Bruker D8 Advance diffractometer equipped with a linear position-sensitive detector (PSD-50m,M. Braun), operating at 40 kV and 40 mA over the range 10–100°. Crystal structure refinement employed the Rietveld method, as implemented in the Fullprof program.[30] The measurements of photoluminescence (PL) and photoluminescence excitation (PLE) spectra were performed by using a Hitachi F7000 spectrometer equipped with a 150 W xenon lamp. In fluorescence lifetime measurements, the third harmonic (355 nm) of a Nd-doped yttrium aluminum garnet laser (Spectra-Physics, GCR130) was used as an excitation source, and the signals were detected with a Tektronix digital oscilloscope (TDS 3052). All the measurements were performed at room temperature.

Acknowledgments

This work was supported by the National Natural Science Foundation of China (NSFC) (grant numbers 10834006, 51172226, 61275055, 11274007, 11174278) and the Natural Science Foundation of Jilin province (grant number 201205024).

[1] J. S. Kim, P. E. Jeon, J. C. Choi, H. L. Park, S. I. Mho, G. C. Kim, *Appl. Phys. Lett.* **2004**, *84*, 2931–2933.
[2] R. J. Xie, N. Hirosaki, T. Suehiro, F. F. Xu, M. Mitomo, *Chem. Mater.* **2006**, *18*, 5578–5583.
[3] W. B. Im, Y. I. Kim, N. N. Fellows, H. Masui, G. A. Hirata, S. P. Den, B. R. Seshadri, *Appl. Phys. Lett.* **2008**, *93*, 091905.
[4] T. Nishida, T. Ban, N. Kobayashi, *Appl. Phys. Lett.* **2003**, *82*, 3817–3819.
[5] M. S. Shur, A. Žukauskas, *Proc. IEEE* **2005**, *93*, 1691–1703.
[6] F. Wang, X. Xue, X. Liu, *Angew. Chem.* **2008**, *120*, 920; *Angew. Chem. Int. Ed.* **2008**, *47*, 906–909.
[7] Y. Uchida, T. Taguchi, *Opt. Eng.* **2005**, *44*, 124003.
[8] V. Bachmann, C. Ronda, A. Meijerink, *Chem. Mater.* **2009**, *21*, 2077–2084.
[9] S. Nakamura, G. Fasol, *The Blue Laser Diode*, Springer, Berlin, **1996**.
[10] S. Nakamura, *MRS Bull.* **2009**, *34*, 101–107.
[11] H. S. Jang, Y. H. Won, D. Y. Jeon, *Appl. Phys. B: Laser Opt.* **2009**, *95*, 715–720.
[12] A. A. Setlur, W. J. Heward, Y. Gao, A. M. Srivastava, R. G. Chandran, M. V. Shankar, *Chem. Mater.* **2006**, *18*, 3314–3322.
[13] Z. Xia, J. Zhuang, L. Liao, H. Liu, Y. Luo, P. J. Du, *J. Electrochem. Soc.* **2011**, *158*, J359–J362.
[14] X. Zhang, L. Fei, J. Shi, M. Gong, *Physica B* **2011**, *406*, 2616–2620.
[15] N. Guo, W. Lü, Y. C. Jia, W. Z. Lv, Q. Zhao, H. P. You, *ChemPhysChem* **2013**, *14*, 192–197.
[16] Y. S. Tang, S. F. Hu, C. C. Lin, N. C. Bagkar, R. S. Liu, *Appl. Phys. Lett.* **2007**, *90*, 151108.
[17] N. Guo, H. P. You, Y. H. Song, M. Yang, K. Liu, Y. H. Zheng, Y. J. Huang, H. J. Zhang, *J. Mater. Chem.* **2010**, *20*, 9061–9067.
[18] Z. C. Wu, J. Liu, W. G. Hou, J. Xu, M. L. Gong, *J. Alloys Compd.* **2010**, *498*, 139–142.
[19] C. H. Huang, Y. C. Chen, T. M. Chen, T. S. Chan, H. S. Sheu, *J. Mater. Chem.* **2011**, *21*, 5645–5649.
[20] C. H. Huang, D. Y. Wang, Y. C. Chiu, Y. T. Yeh, T. M. Chen, *RSC Adv.* **2012**, *2*, 9130–9134.
[21] C. H. Huang, Y. C. Chiu, Y. T. Yeh, T. S. Chan, T. M. Chen, *ACS Appl. Mater. Interfaces* **2012**, *4*, 6661–6668.
[22] A. A. Belik, F. Izumi, T. Ikeda, M. Okui, A. P. Malakho, V. A. Morozov, B. I. Lazoryak, *J. Solid State Chem.* **2002**, *168*, 237–244.
[23] W. J. Yang, L. Y. Luo, T. M. Chen, N. S. Wang, *Chem. Mater.* **2005**, *17*, 3883–3888.
[24] Y. F. Liu, X. Zhang, Z. D. Hao, X. J. Wang, J. H. Zhang, *Chem. Commun.* **2011**, *47*, 10677–10679.
[25] L. Shi, Y. Huang, H. J. Seo, *J. Phys. Chem. A* **2010**, *114*, 6927–6934.
[26] H. P. You, M. Nogami, *J. Phys. Chem. B* **2004**, *108*, 12003–12008.
[27] P. I. Paulose, G. Jose, V. Thomas, N. V. Unnikrishnan, M. K. R. Warrier, *J. Phys. Chem. Solids* **2003**, *64*, 841–846.
[28] M. Inokuti, F. Hirayama, *J. Chem. Phys.* **1965**, *43*, 1978–1989.
[29] H. P. You, J. L. Zhang, G. Y. Hong, H. J. Zhang, *J. Phys. Chem. C* **2007**, *111*, 10657–10661.
[30] J. Rodríguez-Carvajal, *Physica B* **1993**, *192*, 55–69.

Received: September 18, 2013
Published Online: December 16, 2013

